Peer-reviewed version available at *ARO-THE SCIENTIFIC JOURNAL OF KOYA UNIVERSITY* **2020**, *8*, 15-21; doi:10.14500/aro.10591

Type of the Paper (Article)

Multiparameter spatiotemporal anomalies with some of the strong earthquakes (M > 6:0) in 2018 around the world.

Azad Rasul [1, *]

[1] Department of Geography, Soran University, Kawa Street, Soran 44008, Erbil, Iraq
* Correspondence: azad.rasul@soran.edu.iq or aor4@alumni.le.ac.uk; Tel.: +964-(0)750-735-8574

Abstract

One of the most destructive natural disasters is the earthquake which brings enormous risks to humankind. The objective of the current study was to determine the Earthquake's remote sensing multiparameter (i.e. land surface temperature (LST), air temperature, specific humidity, precipitation and wind speed) spatiotemporal anomaly of many earthquake samples occurred during 2018 around the world. In this research 11 earthquake (M > 6:0) studied (4 samples selected in a land with transparent sky situations, 3 samples in land within cloudy situations and 4 samples in marine earthquakes). The interquartile range (IQR) and mean ± 2σ methods utilized to improve the efficiency of anomalous differences. As a result, based on the IQR method, negative anomaly before the event detected during the daytime in Mexico and during the nighttime in Afghanistan. In addition, a negative outlier of brightness temperature (BT) detected in Alaska before, after and during the event. In contrast, based on IQR and mean ± 2σ positive anomaly detected in precipitation before and after the event in all investigated examples. According to mean ± 2σ, negative anomaly LST, specific humidity, sea surface temperature (SST_100) and wind detected in most examined earthquake samples. In contrast, positive SST_0 anomaly observed in Fiji and Honduras after the earthquake. Our results suggested in marine earthquakes, for earthquake forecasting we can merge a prior negative anomaly in the wind speed and SST_100. Regarding the in land cloudy sky earthquakes, merging anomaly parameters could be the negative prior anomaly in BT, skin temperature, in contrast, a positive anomaly in precipitation. In land transparent sky earthquake, usually negative prior anomalies in air temperature, specific humidity and LST.

Keywords: earthquake, anomaly detection, Google Earth Engine, outliers, interquartile range (IQR), multiparameter, brightness temperature (BT), latent heat flux (LE), land surface temperature, wind speed.

1. Introduction

One of the most destructive natural disasters is the earthquake which brings enormous risks to humankind [1]. International seismology and remote sensing community considered utilizing remote sensing data for monitoring of earthquake is a promising research area [2]. Ground stations data represent the low spatial area, therefore, compared to traditional methods of seismic monitoring, satellite data has many advantages [3]. During 2018, 134 earthquakes (M > 6:0) occurred around the world [4] and 11 of them in different locations selected for this research.

May the sign of coming earthquake be arising during monitoring the temperature of underground water, near-surface air temperature, radon, green gas. Moreover, the dominant parameters of temporal-spatial-magnitude of the earthquake are an anomaly of satellite TIR, temperature and ionosphere disturbances [5]. Tramutoli et al. [6] and Tronin et al. [7] detected up to 5 °C temperature increase before the earthquakes in Italy, Japan and China. An increase in land surface temperature (LST) and a decrease in sea surface temperature (SST) observed in the Gujarat earthquake in India by Ouzounov and Freund [8]. Furthermore, Ouzounov et al. [9] discovered infrared signals like outgoing longwave radiation (OLR)

hotspots several days before some earthquakes near the epicentral. Approximately, 7-8 days before the major earthquake, OLR anomaly can increase 30-45 Wm^{-2} around epicentral areas [10]. Zoran et al. [11] discerned the development of spatiotemporal prior anomaly of LST, OLR and mean air temperature parameters related to strong earthquakes in Romania.

Despite occurred productive research in this field, still, uncertainty and arguments remain about pre-seismic anomaly detection due to some crucial misinterpretations and miss earthquake forecasting [12,2]. The seismic community still not completely accepted seismic precursor because it is not perfectly formed [3]. As Jiao et al. [3] suggested that robustness earthquake forecasting could be intensified by means of utilizing combined application and multiparameter analysis. In this research, we utilize multiple parameters because having an anomaly in many parameters prior to the earthquakes in the same location (in the surface, atmosphere, and ionosphere) make forecasting earthquake more sufficiently reliable and realistic. In order to save time and efforts in processing multiparameter long time series data the code script of cloudy based remote sensing platform Google earth Engine (GEE) prepared and utilized. In addition, because detect earthquake anomaly by means of utilizing only one method of statistic is not robust [13], in this study two methods namely interquartile range and mean ± 2σ utilized to improve the efficiency of anomalous difference.

The objective of the current study was to determine the Earthquake's remote sensing multiparameter spatiotemporal anomaly by means of utilizing GEE with R programming for analysing the data of many earthquake samples occurred during 2018 around the world. Samples of the earthquake from marine, in the land transparent sky and in land cloudy situations considered.

2. Materials and methods

2.1. Data

In this research, many parameters utilized which are available in GEE and anomaly of these parameters probably related to the earthquake (Table 1).

Table 1: Details of the utilized data in the research.

Data	Temporal resolution	Spatial resolution	Start date	End date	ImageCollection ID in GEE	Selected band
Brightness temperature	1 day	0.05 arc degrees	1/1/1988	3/7/2018	NOAA/CDR/AVHRR/SR/V4	BT_CH4
Average latent heat flux	8 days	500 meters	1/1/2001	2/26/2018	MODIS/006/MOD16A2	LE
Daytime LST (Terra)	1 day	1000 meters	1/1/2003	2/26/2018	MODIS/006/MOD11A1	LST_Day_1km
Nighttime LST (Terra)	1 day	1000 meters	1/1/2003	2/26/2018	MODIS/006/MOD11A1	LST_Night_1km
Daytime LST (Aqua)	1 day	1000 meters	1/1/2003	2/26/2018	MODIS/006/MYD11A1	LST_Day_1km
Nighttime LST (Aqua)	1 day	1000 meters	1/1/2003	2/26/2018	MODIS/006/MYD11A1	LST_Night_1km
Total precipitation rate	3 hours	0.25 arc degrees	1/1/2000	3/7/2018	NASA/GLDAS/V021/NOAH/G025/T3H	Rainf_f_tavg
Sea water salinity at a depth of 100m	1 day	0.08 arc degrees	1/1/1993	1/21/2018	HYCOM/GLBu0_08/sea_temp_salinity	salinity_0
Average surface skin temperature	3 hours	0.25 arc degrees	1/1/2000	3/7/2018	NASA/GLDAS/V021/NOAH/G025/T3H	AvgSurfT_inst
Specific humidity	3 hours	0.25 arc degrees	1/1/2000	2/26/2018	NASA/GLDAS/V021/NOAH/G025/T3H	Qair_f_inst
Sea water temperature at a depth of 0m	1 day	0.08 arc degrees	1/1/1993	8/29/2018	HYCOM/GLBu0_08/sea_temp_salinity	sst_0
Sea water temperature at a depth of 100m	1 day	0.08 arc degrees	1/1/1993	8/29/2018	HYCOM/GLBu0_08/sea_temp_salinity	sst_100
Air temperature	3 hours	0.25 arc degrees	1/1/2000	2/26/2018	NASA/GLDAS/V021/NOAH/G025/T3H	Tair_f_inst
Wind speed at 10m	3 hours	0.25 arc degrees	1/1/2001	1/21/2018	NOAA/CDR/ATMOS_NEAR_SURFACE/V2	wind_speed

2.2. Study sites

In this research, 11 earthquakes studied which occurred during 2018 around the world (Table 2). Included earthquakes are higher than 6 magnitude. Because earthquakes occurred in different locations and situations, 4 samples selected in the land with transparent sky situations, 3 samples in land within cloudy situations and 4 samples in marine earthquakes. The reason of that firstly is cloudy conditions is the significant problem for active remote sensing data and secondly, the availability of some data is different between the land and the sea.

Table 2: Details of the studied earthquakes.

S.N.	Location	Date	Epicentre	Situation	Magnitude (USGS)	Focal Depth (km, USGS)
1	San Pedro Jicayan, Mexico	16/02/2018	16.386 N, 97.979 W	Land sunny	7.2	22
2	Carandayti, Bolivia	2/4/2018	20.659 S, 63.006 W	Land sunny	6.8	559
3	Iberia, Peru	24/08/2018	11.042 S, 70.817 W	Land sunny	7.1	630
4	Jarm, Afghanistan	31/01/2018	36.526 N, 70.851 E	Land sunny	6.2	193.7
5	Kimble, Papua New Guinea	26/03/2018	151.403 E, 5.502 S	Land cloudy	6.7	40
6	Porgera, Papua New Guinea	25/02/2018	6.070 S, 142.754 E	Land cloudy	7.5	25.2
7	Kaktovik, Alaska, US	12/8/2018	69.562 N, 145.300 W	Land cloudy	6.3	2.2
8	Ndoi Island, Fiji	19/08/2018	178.154 W, 18.113 S	Marine	8.2	600
9	Great Swan Island, Honduras	10/1/2018	83.520 W, 17.483 N	Marine	7.5	19
10	Misawa, Japan	24/01/2018	142.432 E, 41.103 N	Marine	6.3	31
11	Kodiak, Alaska, US	23/01/2018	149.166 W, 56.004 N	Marine	7.9	14.1

2.3. Methodology

Multi parameters (Table 1) processed in GEE (Appendix A)[14]. The ID of data collection and interested band selected. Then date of data selected with “filterDate” one month of data selected with filter Julian day of the year. Images cropped to study site with "filterBounds" and name of the shapefile. Values are multiplied by scale factor if it is required. Then data exported as CSV file.

The data of variables gap filled based on average. Files opened in R programming and anomaly detected and graphs created by means of utilize packages such as "anomalize", "devtools", "tidyverse", "coindeskr", "dplyr" and "ggplot2" (Appendix B).

To detect anomalies in the time series of the data, two methods utilized. The first one is the interquartile range (IQR) which utilize a range of 25 the median [15]. And the second method is mean ± 2σ (equation 1). In this rule, 95% of values drop between [mean-2*σ, mean+2*σ] [16].

$$Anomaly = mean \pm (2\sigma) \qquad (1)$$

For a spatial variation of the centre of the earthquake with its surrounding areas, one buffer with 5 km around the center of earthquake created as the area of the event and 50 km buffer shapefile created around the centre of the earthquake to represent the surrounding areas of the event. Then data of 20 days before and 10 days after the main quake compared between the area of the event and its surrounding areas.

3. Results

3.1. Land earthquake:

As Figure 1 (a: i) indicates no temporal anomaly detected even before and after the event, according to IQR method in specific humidity, latent heat flux (LE) and air temperature in case of Mexico, Bolivia and Peru earthquake samples. However, based on mean ± 2σ method, negative outliers found in specific humidity in both Mexico and Bolivia while positive outlier found in Peru before the earthquake. In terms of LE, no anomaly detected. Positive air temperature anomaly found in Mexico and negative anomaly air temperature detected before the earthquake in both Bolivia and Peru samples (Figure 1j: 1r).

With regard to spatial variation between the location of the earthquake and its surrounding area, in specific humidity of Bolivia and Peru, there were no enormous differences between the two areas. While, in Mexico earthquake, generally the value of the surrounding was higher than the center of the event, however, before the event in second and twelve of February the situation is reversed (Figure 1j).

Generally, the LE of the surrounding areas was higher than the center of the event in both Mexico and Bolivia samples even before and after the day of the event. However, in the Peru earthquake, before the event, in 5th August 2018, LE of the center of the area reversed and reached 0.005 and after that LE of the surrounding area increased (Figure 1o).

In Mexico case, generally, air temperature of the area of the event was higher and in the Peru case, the difference between the location of the event and its surrounding was diminutive. While, in the Bolivia sample, generally, air temperature of the area of the event was higher, however, during 18th of March which is two weeks before the event, air temperature of the area of event decreased compared to the surrounding area. After that, in six days after the event, the situation is reversed (Figure 1p).

Preprints (www.preprints.org) | NOT PEER-REVIEWED | Posted: 9 January 2019 doi:10.20944/preprints201901.0083.v1

Peer-reviewed version available at *ARO-THE SCIENTIFIC JOURNAL OF KOYA UNIVERSITY* **2020**, *8*, 15-21; doi:10.14500/aro.10591

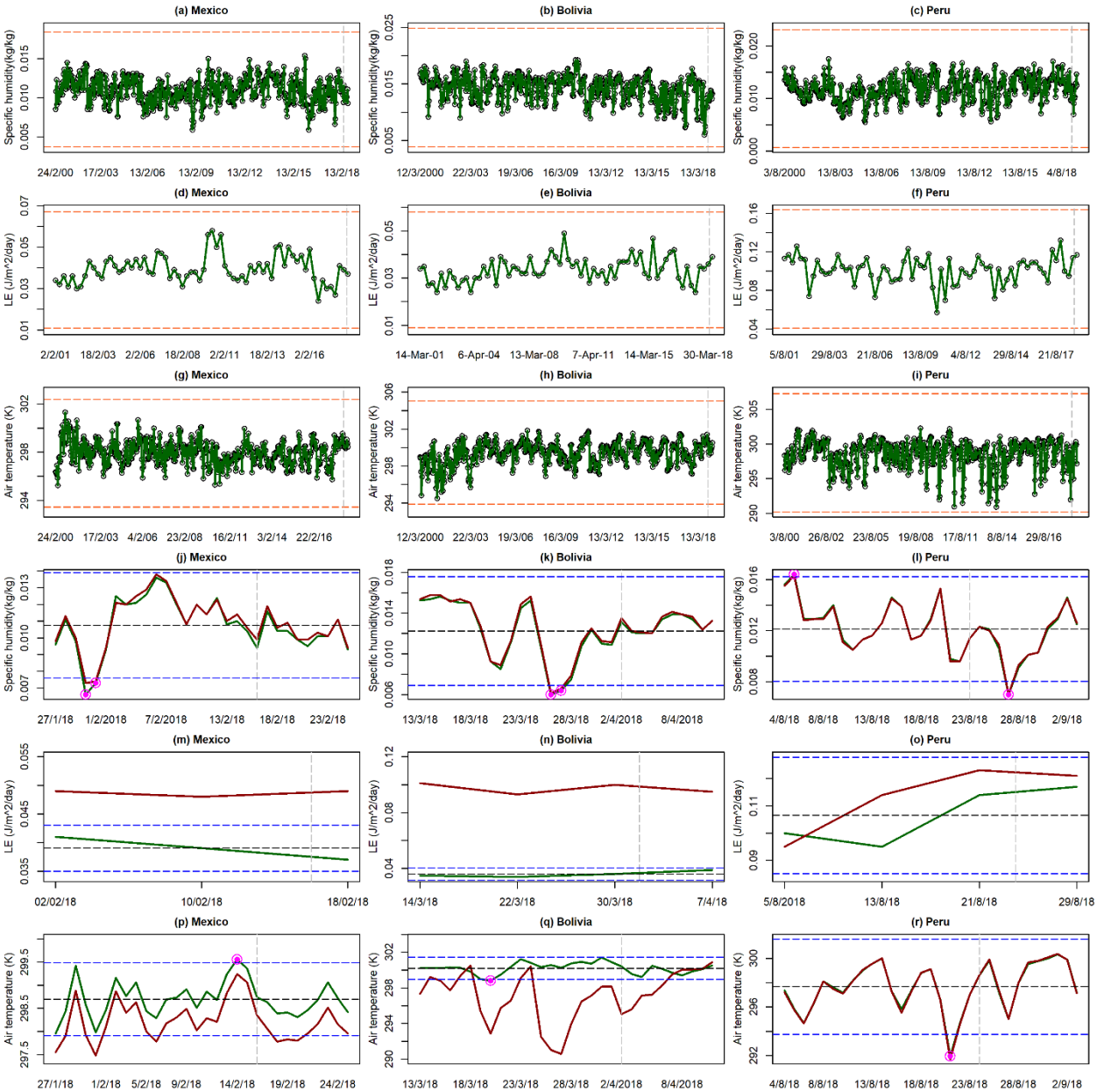

Figure 1: Spatiotemporal anomalies of specific humidity, LE and air temperature in San Pedro Jicayan, Mexico earthquake (16/02/2018), Carandayti, Bolivia earthquake (2/4/2018) and Iberia, Peru earthquake (24/08/2018). Gray dashed line: the day of the earthquake, green line: 5km around the epicenter, red line: 50km areas surrounding epicenter, blue dashed lines: limit-upper and limit-lower based on mean ± 2σ, red dashed lines: limit-upper and limit-lower based on IQR method, magenta circles: anomaly based on mean ± 2σ, black dashed line: mean value of 5km area.

3.1.1. LST anomaly (land earthquake)

Temporal anomaly:

With regard to LST Aqua of both day and night data in Mexico, Bolivia and Afghanistan earthquakes, no anomaly detected before and after the event. In Terra daytime, no outliers detected based on IQR method while in Mexico sample, during the 1st of February which is means 15 days before the event, negative anomaly in LST detected and it is decreased to 295.3K (Figure 2c). In LST Terra nighttime, anomaly not

Preprints (www.preprints.org) | NOT PEER-REVIEWED | Posted: 9 January 2019 doi:10.20944/preprints201901.0083.v1

Peer-reviewed version available at *ARO-THE SCIENTIFIC JOURNAL OF KOYA UNIVERSITY* **2020**, *8*, 15-21; doi:10.14500/aro.10591

detected in Mexico and Bolivia, however, in Afghanistan anomaly detected in 29th of January which means two days before the earthquake occurred and LST of the area of event decreased to 244.6 K (Figure 2l).

According to mean ± 2σ, negative anomaly LST detected before and after in Aqua and Terra data in Mexico, Bolivia and Afghanistan earthquakes, however, only in LST Terra day in Afghanistan positive anomaly detected before the day of the earthquake (Figure 2m: 2x).

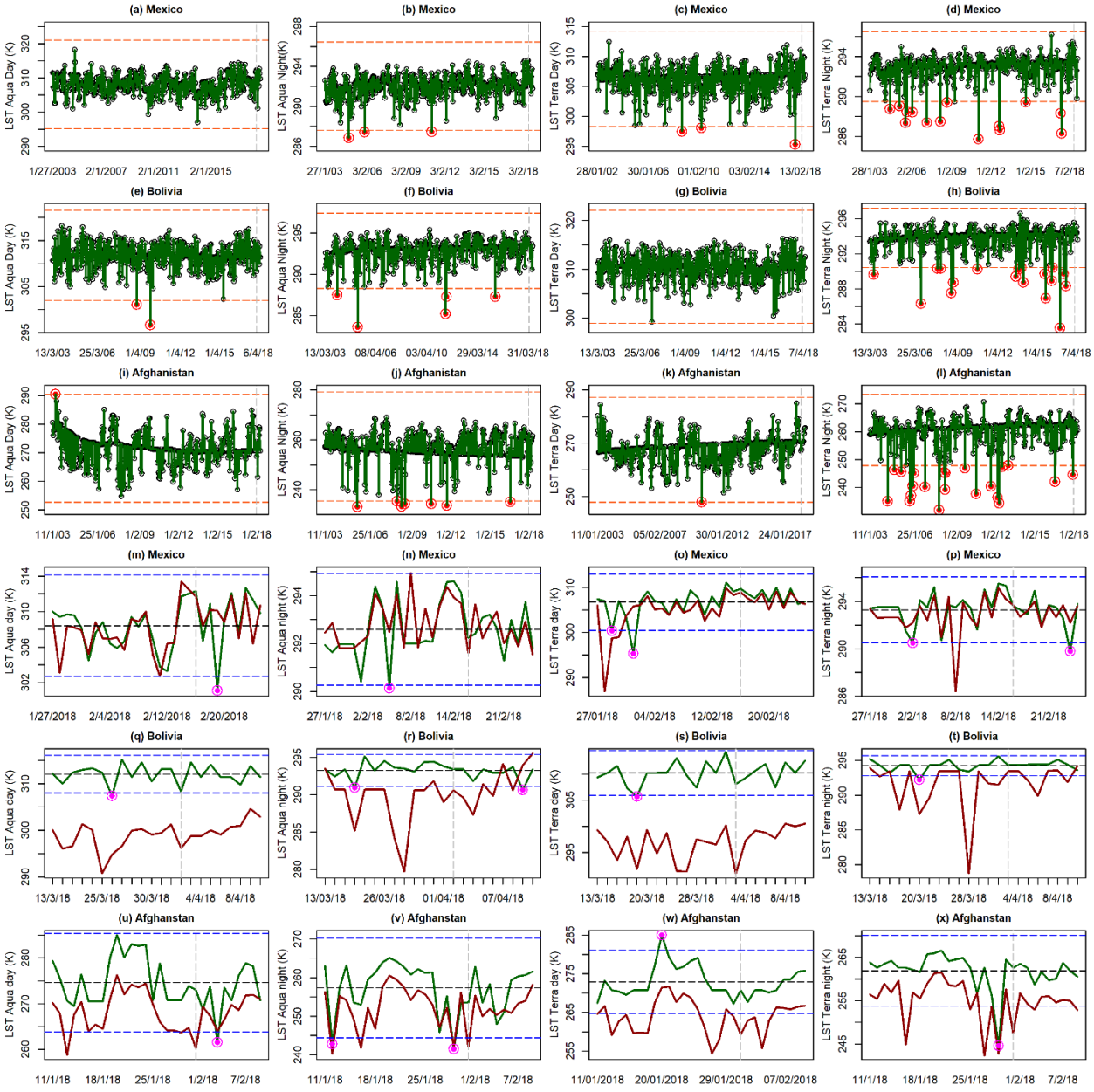

Figure 2: Spatiotemporal anomalies of LST Aqua day, LST Aqua night, LST Terra day, LST Terra night, in San Pedro Jicayan, Mexico earthquake (16/02/2018), Carandayti, Bolivia earthquake (2/4/2018) and Jarm, Afghanistan earthquake (31/01/2018). Gray dashed line: the day of the earthquake, green line: 5km around epicenter, red line: 50km areas surrounding epicenter, blue dashed lines: limit-upper and limit-lower based on mean ± 2σ, red dashed

lines: limit-upper and limit-lower based on IQR method, magenta circles: anomaly based on mean ± 2σ, red circle: IQR based anomalies, black dashed line: mean value of 5km area.

Spatial anomaly:
In Mexico earthquake, in the examined period (20 days before and 10 days after the event), in LST Aqua and Terra (day and night), fluctuations between the area and surrounding occurred. In Bolivia earthquake, in both Terra and Aqua daytime, generally, LST of the area higher than its surrounding areas. While, in the nighttime, usually, LST of the area higher, however, sometimes before and after the event, LST of the surrounding area increased. In Afghanistan earthquake, in Terra and Aqua daytime data, LST of the area higher, however, in LST Aqua nighttime, usually, center area recorded higher LST, however, some days before and after the event, LST of the epicenter area decreased compared to its surrounding (Figure 2v).

3.2. Cloudy earthquake

3.2.1. Temporal anomaly:
In skin temperature, in all samples (Kimble and Porgera Papua New Guinea and Alaska in the US), no anomaly detected during a month around the day of the earthquake (Figure 3a: 3c).

In precipitation of Kimble earthquake (26th March 2018), positive outlier detected during 15, 16, and 18th of March and the precipitation increased. Especially in 15th of March anomalous variation is very high and precipitation reached 7.99 kg/m^2/s. In the Porgera sample (earthquake of 25 February 2018), an anomaly detected in one day before the event and amount of the precipitation was 4.82 kg/m^2/s (Figure 3e). In Alaska earthquake (12th August 2018) some of the positive outliers detected in precipitation during July and August before and after the event, however, during the same period, outliers occurred during 2016 and 2017 (Figure 3f).

With regards to brightness temperature (BT), in Kimble and Porgera earthquakes in Papua New Guinea, not any anomaly detected. However, in the sample of Alaska (earthquake of 12th August 2018) negative anomaly occurred before and after the event and even during the day of the event and BT of the area decreased (Figure 3i).

According to mean ± 2σ, negative anomaly skin temperature only observed in Porgera Papua before the earthquake. Regarding precipitation, a positive anomaly detected before the earthquake in Kimble and Porgera Papua while in Alaska positive anomaly detected before and after the event. Negative outlier BT observed before the vent in Kimble Papua New Guinea and after the event in Porgera (Figure 3j: 3r).

Preprints (www.preprints.org) | NOT PEER-REVIEWED | Posted: 9 January 2019 doi:10.20944/preprints201901.0083.v1

Peer-reviewed version available at *ARO-THE SCIENTIFIC JOURNAL OF KOYA UNIVERSITY* **2020**, *8*, 15-21; doi:10.14500/aro.10591

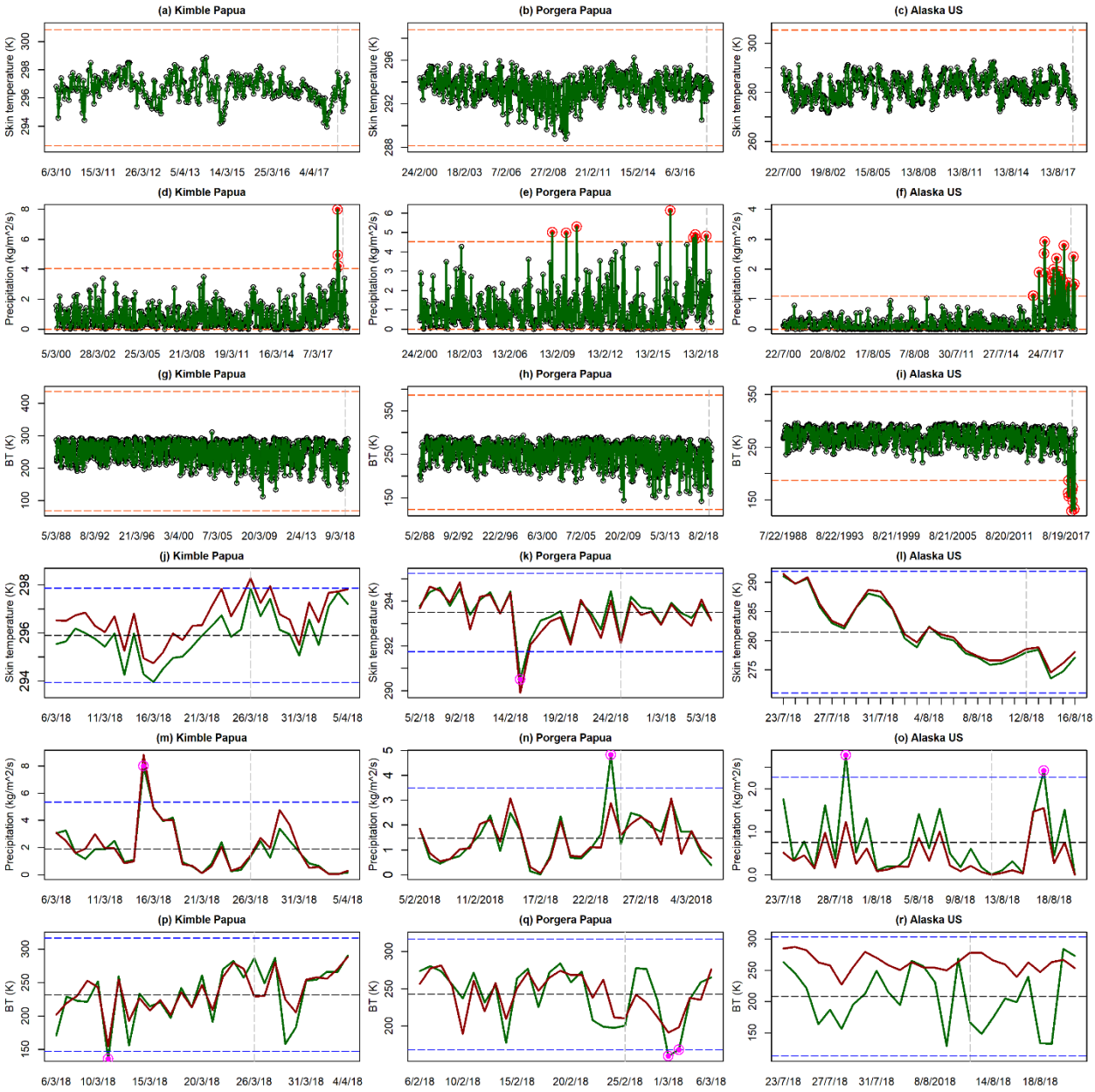

Figure 3: Spatiotemporal anomalies of skin temperature, precipitation and BT, in Kaktovik, Alaska, US earthquake (12/8/2018), Porgera earthquake (25/02/2018) and Kimble, Papua New Guinea (26/03/2018). Gray dashed line: the day of the earthquake, green line: 5km around epicenter, red line: 50km areas surrounding epicenter, blue dashed lines: limit-upper and limit-lower based on mean ± 2σ, red dashed lines: limit-upper and limit-lower based on IQR method, purple circles: anomaly based on mean ± 2σ, red circle: IQR based anomalies, black dashed line: mean value of 5km area.

3.2.2. Spatial anomaly:

In Kimble and Alaska earthquakes, skin temperature of the surrounding areas of the event was higher than the value of center area of the event, however, in the case of Porgera fluctuations occurred between the LST of the area and surrounding areas (Figure 3k).

About spatial differences of precipitation between the area of the event and its surrounding areas, in Alaska, usually, the value of the area was higher, however, in Kimble and Porgera earthquakes, usually, the value of the surrounding areas was higher, however, an anomaly detected before and after the day of the event. Especially, during the 24th of February which is one day before the earthquake, precipitation in the area increased rapidly and reached 4.82 kg/m^2/s while in the surrounding area in the same day, it was only 2.88 kg/m^2/s (Figure 3n).

As a result of compare BT between the area of the event and its surrounding area, Figure 3p, 3q demonstrate fluctuation; sometimes the area was higher and sometimes BT of the surrounding was higher. However, in the Alaska sample, usually BT of the surrounding higher than the center of the area of the event, however, in 6, 7, 11 20 and 21st of August BT of the area rose and became higher than BT of the surrounding area.

3.3. Marine earthquake

According to IQR method no any temporal anomaly detected in marine earthquake samples (Fiji, Honduras and Japan), in variables like SST_0, SST_100, salinity and wind speed (Figure 4). With regarding to the spatial difference between the center of the event and its surrounding areas, usually the value of SST_0 of the area of event is higher than its surrounding areas during 20 days before and 10 days after earthquake. The values reversed in Fiji during the day of the earthquake, in Japan before the event and in Honduras after the day of the event, and the values of the surrounding areas rose compared to the center of the event (Figure 5a: 5c).

Usually, the value of SST_100 of the area of event higher than its surrounding areas in Honduras and Japan sample. However, before the day of the earthquake, sometimes the surrounding areas recorded higher value of SST_100. In the case of Fiji, fluctuations occurred between the two areas (Figure 5d: 5f).

With regard to salinity difference between the center of the event and its surrounding areas, in Fiji earthquake, the value of the area was higher, however, during the day before and the day of the earthquake, the value of salinity of the area decreased compared to the salinity of its surrounding areas. In Honduras, the value of the surrounding area was higher, however, before the day of the event, the value is reversed. In Japan earthquake, the salinity of the area was higher, however, some days before the day of the event, the salinity of the center area decreased compared to its surrounding area (Figure 5g: 5i). Regarding the wind speed, the difference between the two areas was diminutive in all three examples of the earthquake and usually, the value of the surrounding areas was higher compared to the wind speed of the center of earthquakes (Figure 5j: 5i).

According to mean ± 2σ, positive SST_0 anomaly observed in Fiji and Honduras only after the earthquake. While negative SST_100 observed before and after the event in the mentioned samples. Regarding salinity, no any anomaly detected. In addition, negative wind outlier detected before the event in Alaska US and Honduras (Figure 5a: 5i).

Preprints (www.preprints.org) | NOT PEER-REVIEWED | Posted: 9 January 2019 doi:10.20944/preprints201901.0083.v1

Peer-reviewed version available at *ARO-THE SCIENTIFIC JOURNAL OF KOYA UNIVERSITY* **2020**, *8*, 15-21; doi:10.14500/aro.10591

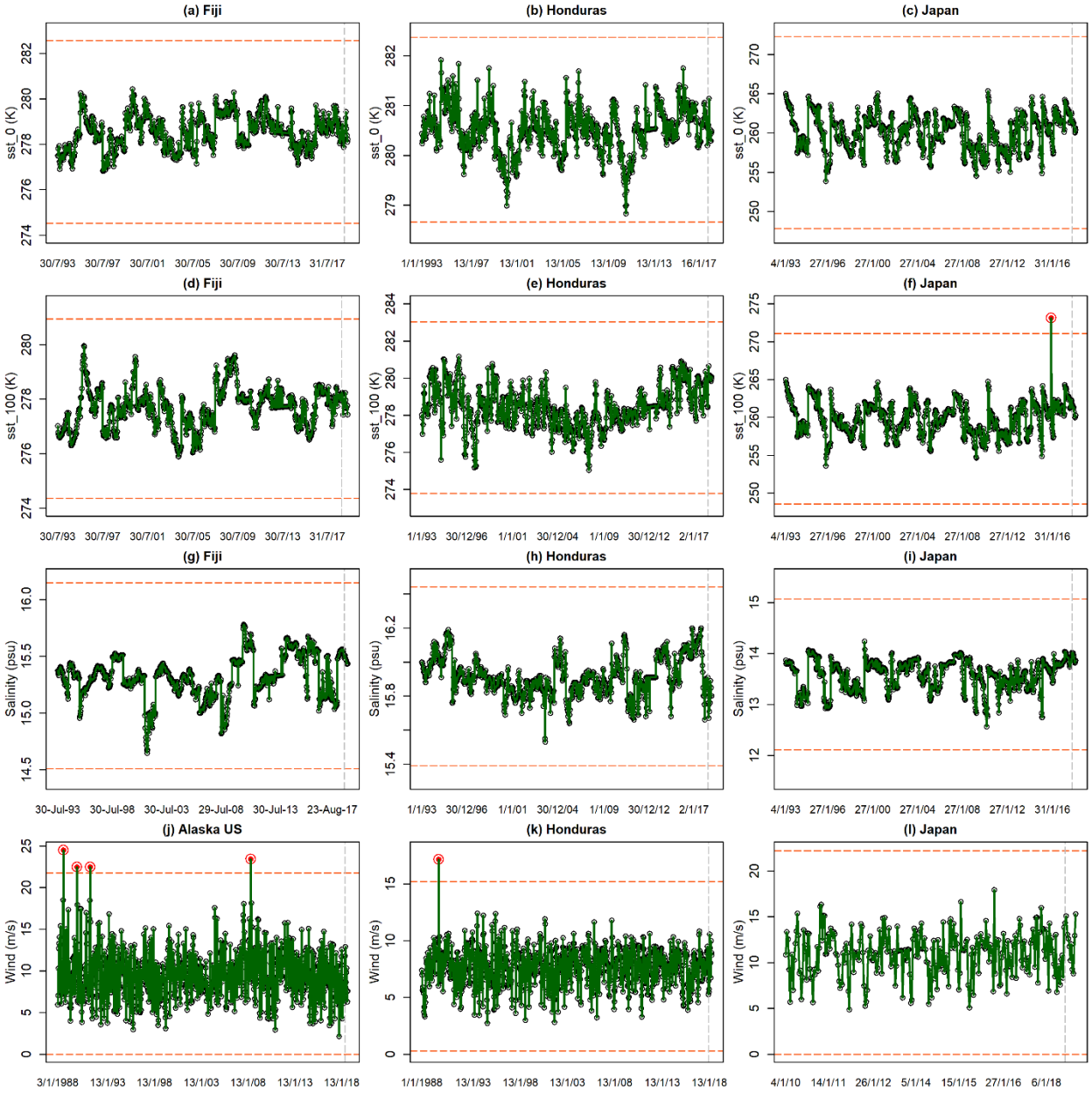

Figure 4: Temporal anomalies of SST_0, SST_100, salinity and wind speed, in Ndoi Island, Fiji earthquake (19/08/2018), Great Swan Island, Honduras earthquake (10/1/2018), Misawa, Japan earthquake (24/01/2018) and Kodiak, Alaska, US earthquake (23/01/2018). Gray dashed line: the day of the earthquake, red dashed lines: limit-upper and limit-lower based on IQR method, red circle: IQR based anomalies.

Preprints (www.preprints.org) | NOT PEER-REVIEWED | Posted: 9 January 2019 doi:10.20944/preprints201901.0083.v1

Peer-reviewed version available at *ARO-THE SCIENTIFIC JOURNAL OF KOYA UNIVERSITY* **2020**, *8*, 15-21; doi:10.14500/aro.10591

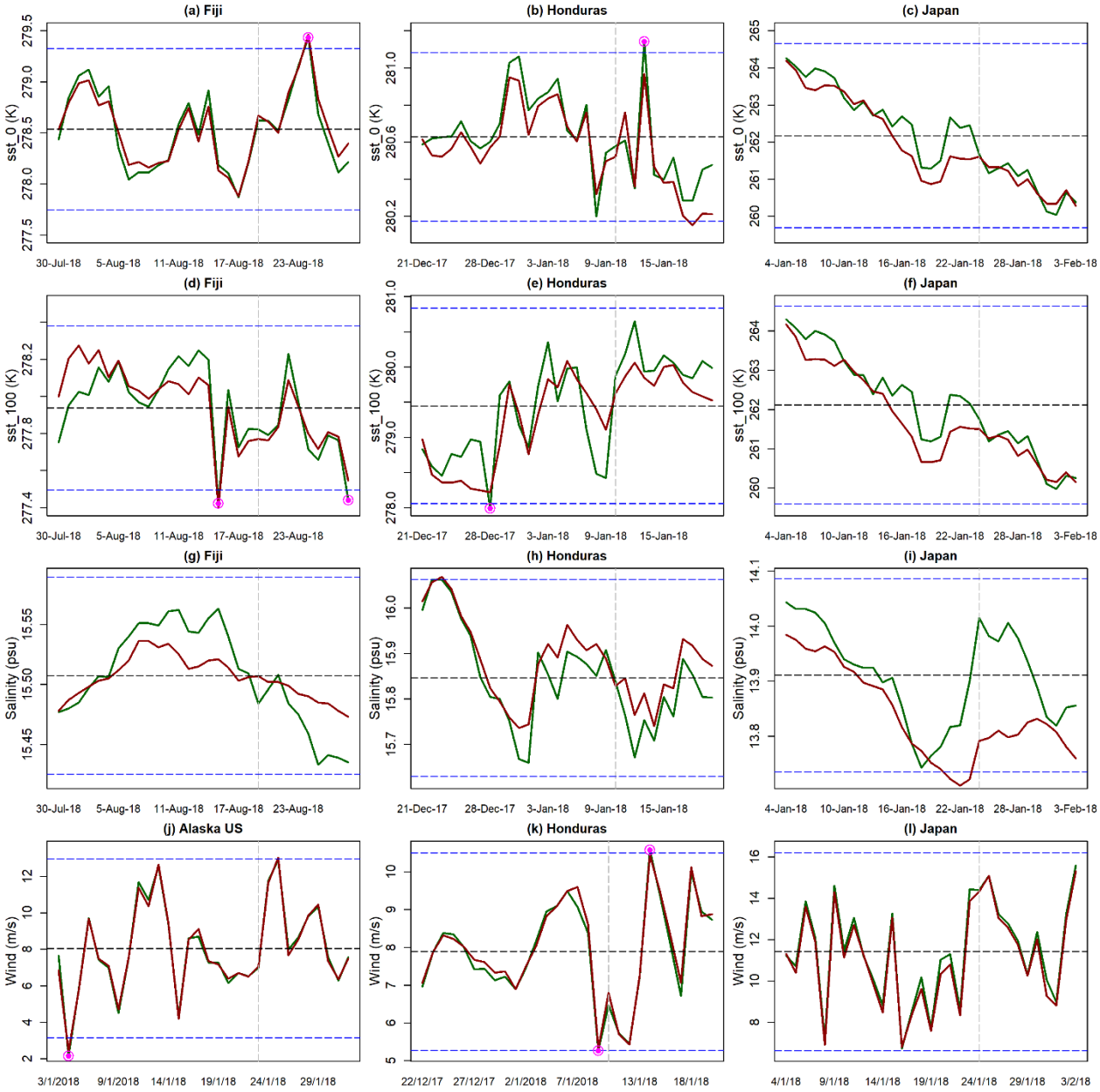

Figure 5: Spatiotemporal anomalies of SST_0, SST_100, salinity and wind speed, in Ndoi Island, Fiji earthquake (19/08/2018), Great Swan Island, Honduras earthquake (10/1/2018), Misawa, Japan earthquake (24/01/2018) and Kodiak, Alaska, US earthquake (23/01/2018). Gray dashed line: the day of the earthquake, green line: 5km around the epicenter, red line: 50km areas surrounding epicenter, blue dashed lines: limit-upper and limit-lower based on mean ± 2σ, magenta circles: anomaly based on mean ± 2σ, black dashed line: mean value of 5km area.

4. Discussions

In LST Terra nighttime, in Afghanistan negative anomaly detected in 29th of January which means two days before the earthquake occurred (Figure 2l), however, during this period of time not only during 2018 outlier detected, however, it occurred during 2006, 2007, 2010, 2012, 2013 and 2017. It implies that perhaps occurring anomaly in LST during this period not completely related to the earthquake. In addition, positive outlier precipitation detected prior of Kimble and Porgera earthquakes, however, during

February 2016, anomaly additionally occurred and it has the possibility to not associated with the earthquake.

In LE parameter by means of utilizing both statistical methods for all examined samples (Mexico, Bolivia and Peru earthquake) no any anomaly observed. Moreover, no anomalies detected in Salinity parameter in the marine earthquake in Fiji, Honduras and Japan (Figure4, 5g: 5i). In SST_0 parameter, only after the earthquake outlier detected (Fiji and Honduras earthquake Figure 5a: 5c) which not useful for earthquake forecasting, however, in SST_100 parameter, before the earthquake anomalies detected (in Fiji and Honduras earthquake) which is more useful for warning residents living near the beach and perhaps they affected by the quake and it may create tsunami.

As a result of comparison 5km around the epicenter to 50km surrounding areas, usually, the value of air temperature, LST, SST_0 and SST_100 parameters higher than the value of the surrounding areas, however, in some points an adverse situation occurred and the value of the center area decreased compared to surrounding areas. Therefore, this can be considered as spatial anomaly before or after the earthquake. However, this method of spatial comparison has a restriction that not all earthquakes similarly affect same amount of area and the effected area not every time take the circle shape.

The anomaly of some parameter is convoluted, regarding specific humidity, two negative anomalies found for each sample of Mexico and Bolivia in contrast positive anomaly found in Peru earthquake (Figure 1j: l). The same result in air temperature observed, diverge from [17] prior negative anomalies detected in Bolivia and Peru earthquake, however, positive anomaly discovered before Mexico earthquake. In LST parameter, usually, a negative anomaly detected while only in LST Aqua daytime in Afghanistan (Figure2i), a positive anomaly discovered.

In marine earthquakes, we can combine two parameters for earthquake forecasting which are a negative anomaly in the wind speed and SST_100 based on mean ± 2σ during 20 days before the main quake. While after the event, the positive anomaly may occur in SST_0 and wind speed. Regarding the in land cloudy sky earthquakes, which create an issue for many remote sensing data, combining anomaly parameters could be the negative anomaly in BT, skin temperature, in contrast, a positive anomaly in precipitation during 20 days prior the main quake. During 10 days after the main quake, a negative anomaly in BT and a positive anomaly in precipitation perhaps occur. In land transparent sky earthquake, an anomaly in some parameters perhaps assist to forecast the earthquake such as, usually, negative (perhaps positive) anomaly in air temperature, usually negative (and perhaps positive) anomaly in specific humidity according to mean ± 2σ method. Regards to LST, diverge from [18,19] usually negative (and perhaps positive (Figure 2i, 2w)) anomalies during 20 days before the earthquake. After the earthquake during 10 days, a negative anomaly in both Aqua and Terra LST and specific humidity could be anticipated.

As a result of investigated 11 samples of an earthquake during 2018, we discerned in some earthquakes, anomaly in more than one parameter discerned such as Mexico, Bolivia, Peru, Honduran and Fiji. In contrast, in Japan earthquake anomaly not detected in any parameters.

5. Conclusion

The aim of the current study was to determine the Earthquake's remote sensing multiparameter spatiotemporal anomaly of many earthquake samples occurred during 2018 around the world. Samples of the earthquake from marine, in the land transparent sky and in land cloudy situations considered.

Peer-reviewed version available at ARO-THE SCIENTIFIC JOURNAL OF KOYA UNIVERSITY 2020, 8, 15-21; doi:10.14500/aro.10591

Multi-parameters (i.e. LST, air temperature, specific humidity, SST, precipitation and wind speed) which available through GGE and they may be related to the earthquake utilized and analysed by means of utilizing of GEE with R programming.

As a result, based on the IQR method, negative anomaly before the event detected during the daytime in Mexico and during the nighttime detected in Afghanistan. In addition, a negative outlier of BT detected in Alaska before, after and during the event. In contrast, based on IQR and mean ± 2σ positive anomaly detected in precipitation before and after the event in all investigated examples. According to mean ± 2σ, negative anomaly LST, specific humidity, SST_100 and wind detected in most examined earthquake samples. In contrast, positive SST_0 anomaly discerned in Fiji and Honduras after the earthquake.

With regard to spatial variation between the location of the earthquake and its surrounding area, in specific humidity in Mexico earthquake and LE of Peru earthquake, before the event, the value of the center of the area increased. In LST Aqua nighttime usually area recorded higher LST however, some days before and after the event, LST of the area decreased compared to its surrounding. In Kimble and Porgera earthquake, usually precipitation of the surrounding was higher however, an anomaly detected before and after the day of the event. Before and after or during the day of the earthquake, the values of SST_0 and SST_100 decreased compared to surrounding areas.

In marine earthquakes, we can merge two parameters for earthquake forecasting which are a negative anomaly in the wind speed and SST_100 based on mean ± 2σ before the main quake. Regarding the in land cloudy sky earthquakes, merging anomaly parameters could be the negative anomaly in BT, skin temperature, in contrast, a positive anomaly in precipitation prior to the main quake. In land transparent sky earthquake, an anomaly in some parameters may assist to forecast the earthquake such as usually negative (perhaps positive) anomaly in air temperature, usually negative (and perhaps positive) anomaly in specific humidity according to mean ± 2σ method. Regards to LST, usually negative (and perhaps positive anomalies the same as [11] discerned) before the earthquake.

This study may have some limitations, for instance, the source of some of the utilized data like precipitation is Global Land Data Assimilation System "GLDAS-2.1" which is utilize modeling and data assimilation techniques with satellite and ground-based data. Furthermore, some parameters may be related to the earthquake not included in this study because they were not available on GEE. In addition, and some anomaly detected around the earthquake period, may not relate to the occurred earthquake because of anomalies discerned during the same month of previous years. future research should focus on other reliable factors that may be related to an earthquake within the utilize of more techniques and statistical methods for discovering robust results that may contribute to predict an earthquake in the future.

Funding: This research received no external funding.

Acknowledgments: The author would like to thank the Google Earth Engine program and the R Development Core Team to continuously improve and support this freely available software.

References

1. Geiß, C. & Taubenböck, H. Remote sensing contributing to assess earthquake risk: from a literature review towards a roadmap. *Nat. Hazards* **68**, 7–48 (2013).

2. Tronin, A. Satellite Remote Sensing in Seismology. A Review. *Remote Sens.* **2**, 124–150 (2009).

3. Jiao, Z.-H., Zhao, J. & Shan, X. Pre-seismic anomalies from optical satellite observations: a review. *Nat. Hazards Earth Syst. Sci.* **18**, 1013–1036 (2018).
4. USGS Earthquake Hazards Program. Available at: https://earthquake.usgs.gov/. (Accessed: 5th January 2019)
5. Wu, L. & Liu, S. Remote sensing rock mechanics and earthquake thermal infrared anomalies. in *Advances in Geoscience and Remote Sensing* (IntechOpen, 2009).
6. Tramutoli, V., Di Bello, G., Pergola, N. & Piscitelli, S. Robust satellite techniques for remote sensing of seismically active areas. (2001).
7. Tronin, A. A., Hayakawa, M. & Molchanov, O. A. Thermal IR satellite data application for earthquake research in Japan and China. *J. Geodyn.* **33**, 519–534 (2002).
8. Ouzounov, D. & Freund, F. Mid-infrared emission prior to strong earthquakes analyzed by remote sensing data. *Adv. Space Res.* **33**, 268–273 (2004).
9. Ouzounov, D., Pulinets, S., Kafatos, M. C. & Taylor, P. Thermal Radiation Anomalies Associated with Major Earthquakes. in *Geophysical Monograph Series* (eds. Ouzounov, D., Pulinets, S., Hattori, K. & Taylor, P.) 259–274 (John Wiley & Sons, Inc., 2018). doi:10.1002/9781119156949.ch15
10. Rawat, V., Saraf, A. K., Das, J., Sharma, K. & Shujat, Y. Anomalous land surface temperature and outgoing long-wave radiation observations prior to earthquakes in India and Romania. *Nat. Hazards* **59**, 33–46 (2011).
11. Zoran, M. A., Savastru, R. S. & Savastru, D. M. Satellite thermal infrared anomalies associated with strong earthquakes in the Vrancea area of Romania. *Open Geosci.* **7**, (2015).
12. Geller, R. J. Shake-up time for Japanese seismology. *Nature* **472**, 407–409 (2011).
13. Bhardwaj, A. *et al.* MODIS-based estimates of strong snow surface temperature anomaly related to high altitude earthquakes of 2015. *Remote Sens. Environ.* **188**, 1–8 (2017).
14. Google Earth Engine. Available at: https://earthengine.google.com. (Accessed: 19th November 2018)
15. Dancho, M. & Vaughan, D. *anomalize: Tidy Anomaly Detection*. (2018).
16. Anomaly Detection with the Normal Distribution. *Anomaly* (2015).
17. Alvan, H. V., Azad, F. H. & Mansor, S. Latent heat flux and air temperature anomalies along an active fault zone associated with recent Iran earthquakes. *Adv. Space Res.* **52**, 1678–1687 (2013).
18. Nezammahalleh, M. A. *et al.* IDENTIFICATION OF ACTIVE AREAS OF EARTHQUAKE BY THERMAL REMOTE SENSING. *ISPRS - Int. Arch. Photogramm. Remote Sens. Spat. Inf. Sci.* **XL-1/W3**, 295–299 (2013).

19. Saraf, A. K. *et al.* Detecting Earthquake Precursor: A Thermal Remote Sensing Approach. *Proc. "Map India* (2008).

Appendices

Appendix A: A Sample of process data in the Google Engine Code.

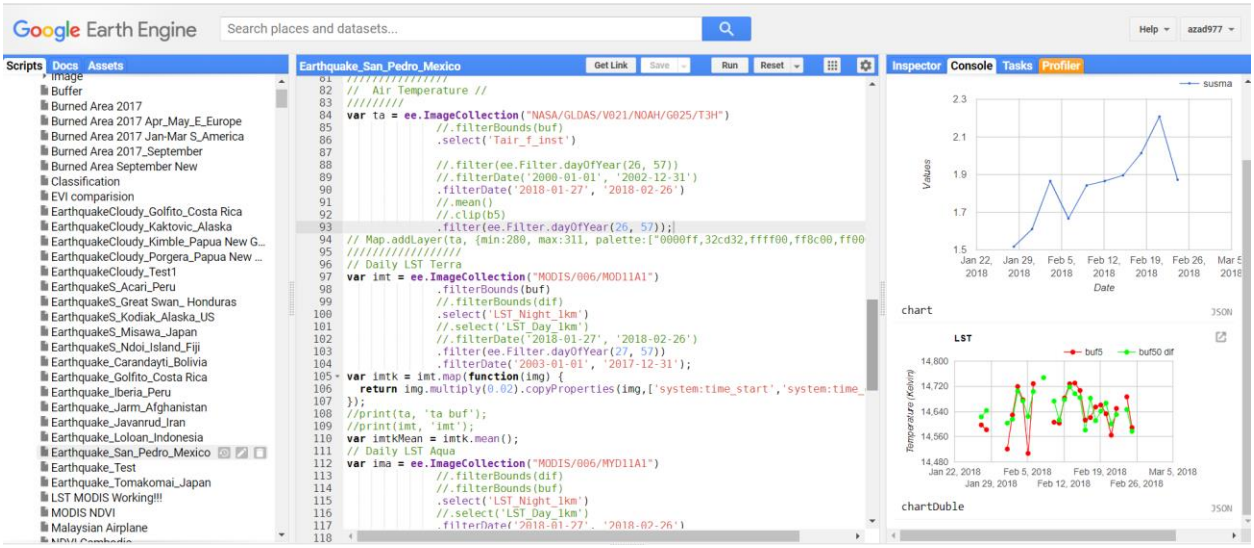

Appendix B: A sample of utilized R code in the study.

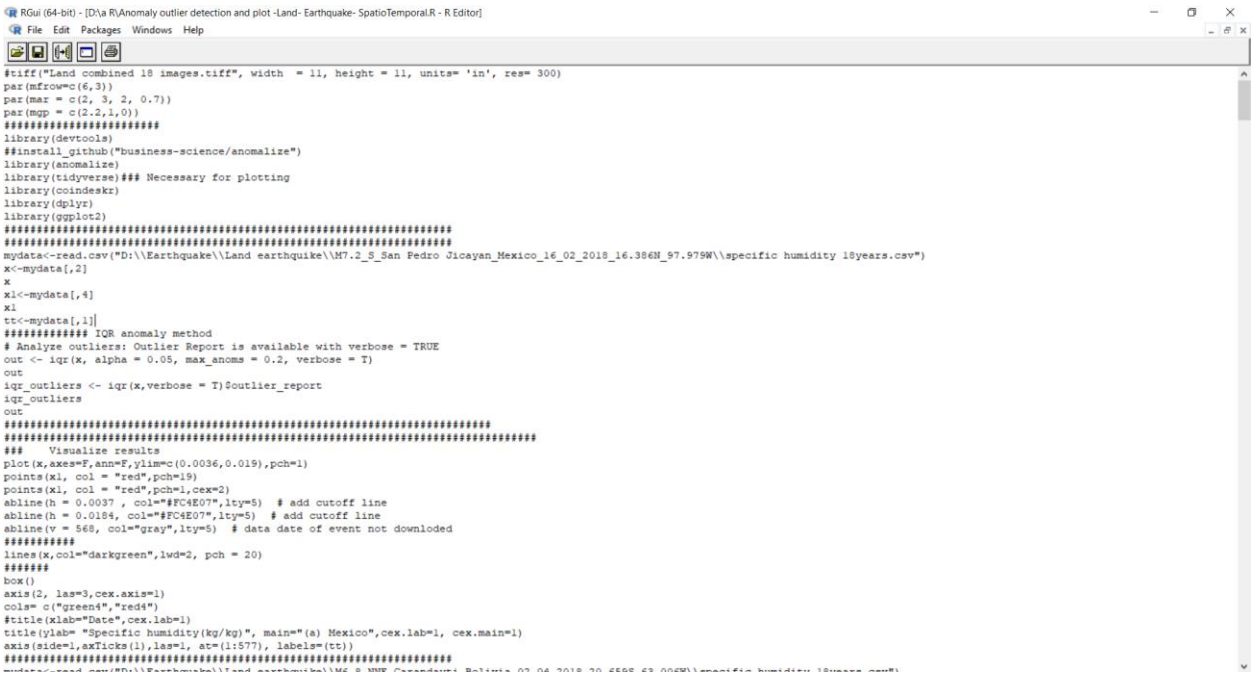


```
#tiff("Land combined 18 images.tiff", width  = 11, height = 11, units= 'in', res= 300)
par(mfrow=c(6,3))
par(mar = c(2, 3, 2, 0.7))
par(mgp = c(2.2,1,0))
########################
library(devtools)
##install_github("business-science/anomalize")
library(anomalize)
library(tidyverse)### Necessary for plotting
library(coindeskr)
library(dplyr)
library(ggplot2)
#########################################################################
#########################################################################
mydata<-read.csv("D:\\Earthquake\\Land earthquike\\M7.2_S_San Pedro Jicayan_Mexico_16_02_2018_16.386N_97.979W\\specific humidity 18years.csv")
x<-mydata[,2]
x
x1<-mydata[,4]
x1
tt<-mydata[,1]
########## IQR anomaly method
# Analyze outliers: Outlier Report is available with verbose = TRUE
out <- iqr(x, alpha = 0.05, max_anoms = 0.2, verbose = T)
out
iqr_outliers <- iqr(x,verbose = T)$outlier_report
iqr_outliers
out
#########################################################################
#########################################################################################
###     Visualize results
plot(x,axes=F,ann=F,ylim=c(0.0036,0.019),pch=1)
points(x1, col = "red",pch=19)
points(x1, col = "red",pch=1,cex=2)
abline(h = 0.0037 , col="#FC4E07",lty=5)  # add cutoff line
abline(h = 0.0184, col="#FC4E07",lty=5)  # add cutoff line
abline(v = 568, col="gray",lty=5)  # data date of event not downloded
###########
lines(x,col="darkgreen",lwd=2, pch = 20)
#######
box()
axis(2, las=3,cex.axis=1)
cols= c("green4","red4")
#title(xlab="Date",cex.lab=1)
title(ylab= "Specific humidity(kg/kg)", main="(a) Mexico",cex.lab=1, cex.main=1)
axis(side=1,axTicks(1),las=1, at=(1:577), labels=(tt))
#########################################################################
```